

Department	Mechanical		Program	B.Tech		
Subject Name	Basic Fracture Mechanics		Subject Code	MEC 701		
Semester	7th	Credits		Teacher Incharge/Mentor		
Name	Junaid Hassan Masoodi		Mobile No.	9596503735	Email	Junaid_phd12@nitsri.net

Unit I: Basic Fracture Mechanics

Topic Name: Basic problems and concepts in fracture mechanics, Crack tip stresses

Links to the Resources:

1. web.mit.edu/course/3/3.11/www/modules/frac.pdf
2. <http://nptel.ac.in/courses/112106065/2>
3. <http://nptel.ac.in/courses/112106065/3>
4. <http://nptel.ac.in/courses/112106065/4>
5. <http://nptel.ac.in/courses/112106065/5>
6. <http://nptel.ac.in/courses/112106065/6>
7. <http://nptel.ac.in/courses/112106065/7>
8. <http://nptel.ac.in/courses/112106065/25>
9. <http://nptel.ac.in/courses/112106065/26>
10. <http://nptel.ac.in/courses/112106065/27>
11. <http://nptel.ac.in/courses/112106065/31>
12. <http://nptel.ac.in/courses/112106065/32>
13. <http://nptel.ac.in/courses/112106065/33>

Lecture Notes:

Lecture 1:

1.1 Introduction

Through the ages the application of materials in engineering design has posed difficult problems to mankind. In the Stone Age the problems were mainly in the shaping of the material. In the early days of the Bronze Age and the Iron Age the difficulties were both in production and shaping. For many centuries metal-working was laborious and extremely costly. Estimates go that the equipment of a knight and horse in the thirteenth century was of the equivalent price of a Centurion tank in World War II.

With the improving skill of metal working, applications of metals in structures increased progressively. Then it was experienced that structures built of these materials did not always behave satisfactorily, and unexpected Failures often occurred. Detailed descriptions of castings and forgings produced in the Middle Ages exist. When judged with present day knowledge, these production methods must have been liable to build important technical deficiencies into the structure.

The vastly increasing use of metals in the nineteenth century caused the number of accidents and casualties to reach unknown levels. The number of people killed in railway accidents in Great Britain was in the order of two hundred per year during the decade 1860-1870. Most of the accidents were a result of derailing caused by

fractures of wheels, axles or rails. Anderson [1] has recently made an interesting compilation of accident reports from the last two hundred years. A few quotations follow:

1. On the 19th of March 1830 about 700 persons assulted on the Montrose suspension bridge to witness a boat race, when one of the main chains gave way ... and caused considerable loss of life."
2. "On the 22nd of January 1866. a portion of the roof of the Manchester railway station fell, causing deaths of two men. The accident was caused by failure of cast-iron struts connected ... "
3. "A high pressure water main burst at Boston. January 3, 1913, and flooded the district. ..
4. "The most serious railroad accident of the week occurred April 20 (1887) and was caused by the breaking of a drawbar. Three were killed and two fatally injured."
5. "The most serious railroad accident of the week occurred May 27 (1887).
6. The bursting of a wheel caused the deaths of six people."
7. "The most serious railroad accident of the week occurred on July 2 (1887) and was caused by the breaking of an axle."

Some of these accidents were certainly due to a poor design, but it was gradually discovered that material deficiencies in the form of pre-existing flaws could initiate cracks and fractures. Prevention of such flaws would improve structural performance. Better production methods together with increasing knowledge and comprehension of material properties led to a stage where the number of failures was reduced to more acceptable levels. A new era of accident prone structures started with the introduction of all-welded designs. Out of 2500 Liberty ships built during World War II. 145 broke in two and almost 700 experienced serious failures. The same disaster struck many bridges and other structures. The failures often occurred under conditions of low stresses (several ships failed suddenly while in the harbour) which made them seemingly inexplicable. As a result extensive investigations were initiated in many countries and especially in the United States or America. This work revealed that here again. flaws and stress concentrations (and to a certain extent internal stresses) were responsible for failure.

The fractures were truly brittle: they were accompanied by very little plastic deformation. It turned out that the brittle fracture of steel was promoted by low temperatures and by conditions of triaxial stress such as may exist at a sharp notch or a flaw. Under these circumstances structural steel can fracture by cleavage without noticeable plastic deformation. Above a certain temperature, called the transition temperature, the steel behaves in a ductile manner. The transition temperature may go up as a result of the heat cycle during the welding process.

At present, brittle fractures of welded structures built out of low strength structural steels can be satisfactorily prevented. It has to be ensured that the material is produced to have a low transition temperature and that the welding process does not raise the ductile-brittle transition. Large stress concentrations should be avoided and the welds should be checked to be virtually free of defects.

After World War II the use of high strength materials has increased considerably. These materials are often selected to realize weight savings. Simultaneously, stress analysis methods were developed which enable a more

reliable determination of local stresses. This permitted safety factors to be reduced resulting in further weight savings. Consequently, structures designed in high strength materials have only low margins of safety. This means that service stresses (sometimes with the aid of an aggressive environment) may be high enough to induce cracks, particularly if preexisting flaws or high stress concentrations are present. The high strength materials have a low crack resistance (fracture toughness): the residual strength under the presence of cracks is low. When only small cracks exist, structures designed in high strength materials may fail at stresses below the highest service stress they were designed for'.

Low stress fractures induced by small cracks are in many aspects very similar to the brittle fractures of welded low-strength steel structures. Very little plastic deformation is involved: the fracture is brittle in all engineering sense, although the micromechanism of separation is the same as in ductile fracture. The occurrence of low stress fracture in high strength materials induced the development of *Fracture Mechanics*.

1.2 A crack in a structure

Consider a structure in which a crack develops. Due to the application of repeated loads or due to a combination of loads and environmental attack this crack will grow with time. The longer the crack, the higher the stress concentration induced by it. This implies that the rate of crack propagation will increase with time. The crack propagation as a function of time can be represented by a rising curve as in Figure 1.1(a). Due to the presence of the crack the strength of the structure is decreased: It is lower than the original strength it was designed for.

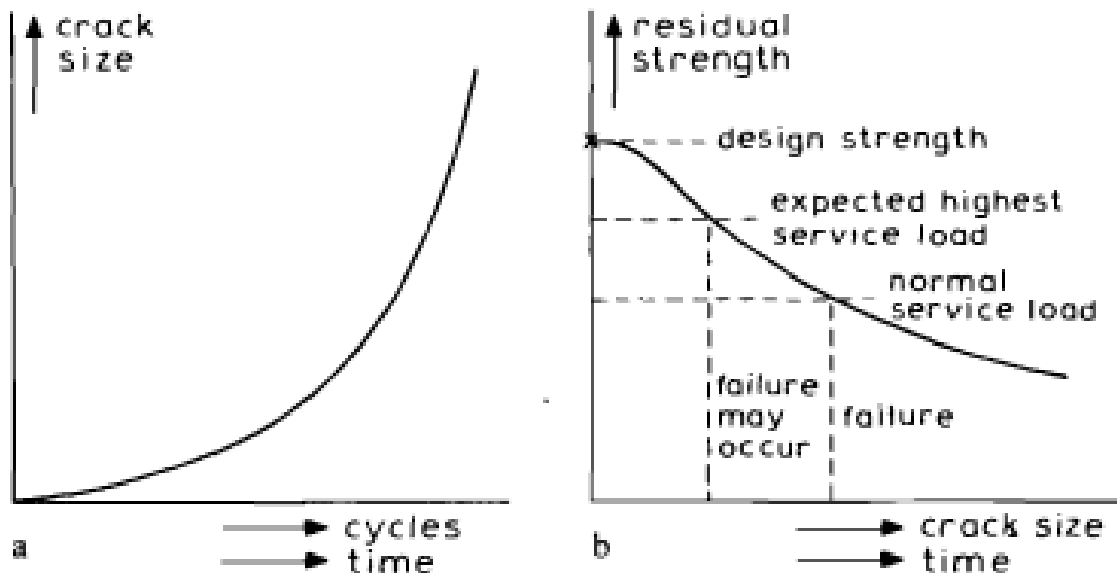


Figure:1.1 The engineering problem (a) Crack growth curve (b) Residual strength curve

The residual strength of the structure decreases progressively with increasing crack size, as is shown diagrammatically in Figure 1.1 (b). After a certain time the residual strength has become so low that the structure cannot withstand accidental high loads that may occur in service. From this moment on the structure is liable to

fail. If such accidental high loads do not occur, the crack will continue to grow until the residual strength has become so low that fracture occur under normal service loading. Many structure are designed to carry service loads that are high enough to initiate cracks particularly when pre-existing news or stress concentration are present. The designer has to anticipate this possibility of cracking and consequently he has to accept a certain risk that the structure will fail. This implies that the structure can have only a limited lifetime. Of course, the probability of failure should be at an acceptably low level during the whole service life. In order to ensure this safety it has to be predicted how fast cracks will grow and how fast the residual strength will decrease: Making these predictions and developing prediction methods are the objects of fracture mechanics.

As depicted in [Figure 1.2](#) several disciplines are involved in the development of fracture mechanics design procedures. At the right end of the scale is the engineering load-and-stress analysis. Applied mechanics provide the crack tip stress fields as well as the elastic and (to a certain extent) plastic deformations of the material in the vicinity of the crack. The predictions made about fracture strength can be checked experimentally. Material Science concerns itself with the fracture processes on the scale of atoms and dislocations to that of impurities and grains. From a comprehension of these processes the criteria which govern growth and fracture should be obtainable. These criteria have to be used to predict the behavior of a crack in a given stress-strain held. An understanding of fracture processes can also provide the material parameters of importance to crack resistance; these have to be known if materials with better crack resistance are to be developed. In order to make a successful use of fracture mechanics in engineering application, it is essential to have some knowledge of the total field of [Figure 1.2](#). This book attempts to provide a basic understanding of this field.

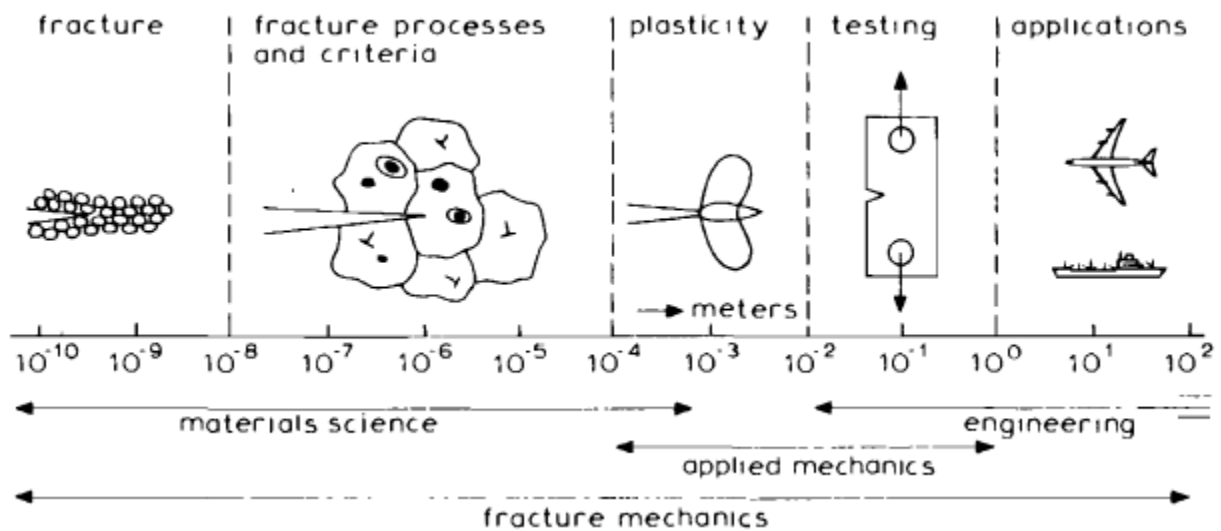


Figure 1.2. The broad field of fracture mechanics

Lecture 2:

1.3 The stress at a crack tip

A crack in a solid can be stressed in three different modes, as illustrated in Figure 1.3. Normal stresses give rise to the "opening mode" denoted as mode I. The displacements of the crack surfaces are perpendicular to the plane

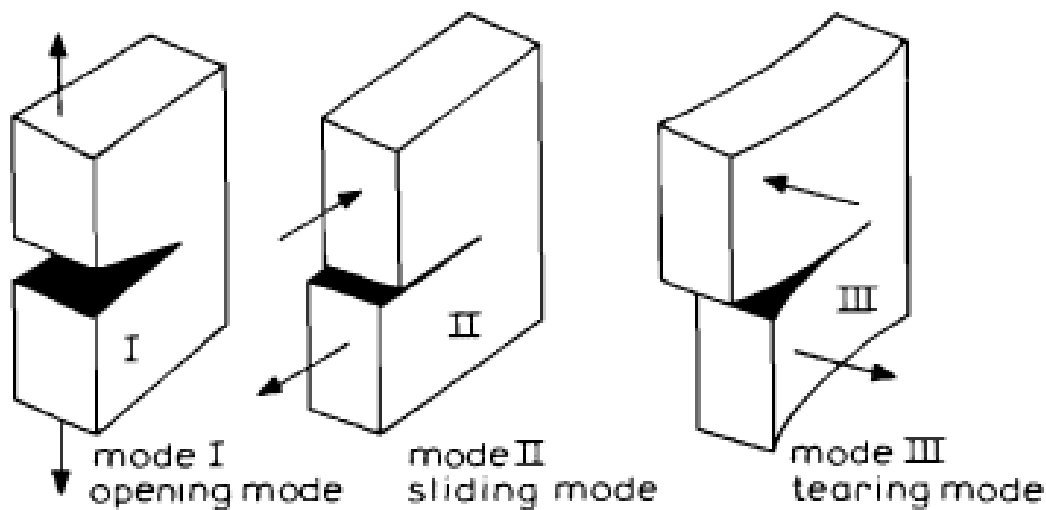


Figure 1.3. The three modes of cracking

or the crack. The displacements of the crack surfaces are perpendicular to the plane or the crack. In-plane shear results in mode II or "sliding mode": the displacement of the crack surfaces is in the plane of the crack and perpendicular to the leading edge of the crack. The "tearing mode" or mode III is caused by out of plane shear. Crack surface displacements are in the plane of the crack and parallel to the leading edge of the crack. The superposition of the three modes describes the general case of cracking.

Consider a through-the-thickness mode I crack of length $2a$ in an infinite plate as in Figure 1.4. The plate is subjected to a tensile stress σ at infinity. An element $dx dy$ of the plate at a distance r from the x and y directions and a shear stress τ_{xy} .

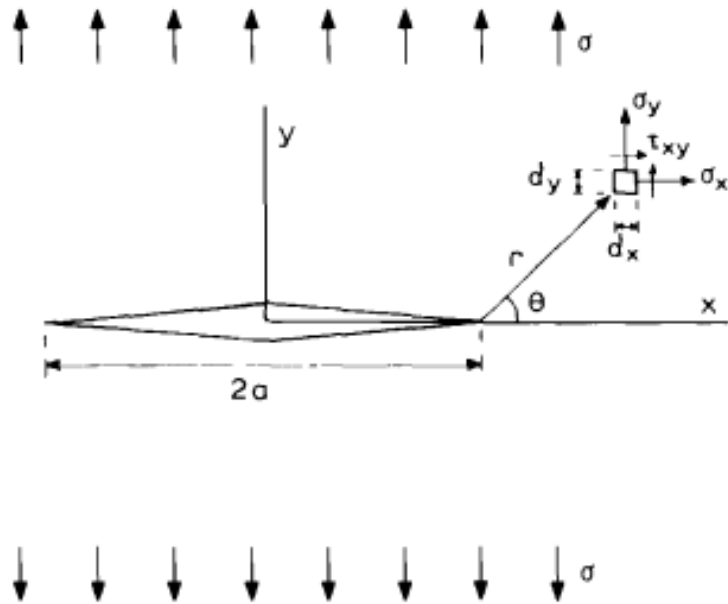


Figure 1.4: Crack in all infinite plate

$$\left\{ \begin{array}{l} \sigma_{xx} = \sigma \sqrt{\frac{a}{2r}} \cos\left(\frac{\theta}{2}\right) \left[1 - \sin\left(\frac{\theta}{2}\right) \cos\left(\frac{3\theta}{2}\right)\right] \\ \sigma_{yy} = \sigma \sqrt{\frac{a}{2r}} \cos\left(\frac{\theta}{2}\right) \left[1 + \sin\left(\frac{\theta}{2}\right) \cos\left(\frac{3\theta}{2}\right)\right] \\ \tau_{xy} = \sigma \sqrt{\frac{a}{2r}} \cos\left(\frac{\theta}{2}\right) \sin\left(\frac{\theta}{2}\right) \cos\left(\frac{3\theta}{2}\right) \\ \sigma_{zz} = 0 \quad \text{(Plane stress (PSS))} \\ \sigma_{zz} = \nu(\sigma_{xx} - \sigma_{yy}) \quad \text{(Plain strain (PSN))} \end{array} \right. \quad (1.1)$$

As should be expected, in the elastic case the stresses are proportional to the external stress σ . They vary with the square root of the crack size and they tend to infinity at the crack tip where r is small. The distribution of the stress σ_{xx} as a function of r at $\theta = 0$ is illustrated in Figure 1.5. For large r the stress σ_{yy} approaches zero, while it should go to σ . Apparently Equation 1.1 are valid only for a limited area around the crack tip. Each of the equations represents the first term of a series. In the vicinity of the crack tip these first terms give a sufficiently accurate description of the crack tip stress fields, since the following terms are small compared to the first.

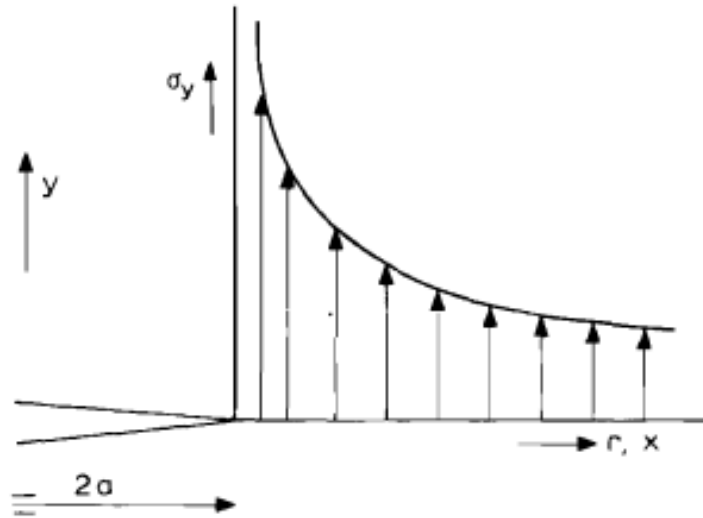


Figure 1.5: Elastic stress at the crack tip

The functions of the coordinates r and θ in Equations (1.1) are explicit. The equation can be written in the generalized form

$$\sigma_{ij} = \left(\frac{K_I}{\sqrt{2\pi r}} \right) f_{ij}(\theta) \quad \text{with } K_I = \sigma\sqrt{\pi a} \quad (1.2)$$

The factor K_I is known as the "stress intensity factor", where the subscript I stands for mode I. The whole stress field at the crack tip is known when the stress intensity factor is known. Two cracks, one of size $4a$ the other of size a have the same stress field at their tips if the first crack is loaded to σ and the other to 2σ . In that event K_I is the same for both cracks. Equation (1.2) is an elastic solution, which does not prohibit that the stresses become infinite at the crack tip. In reality this cannot occur: plastic deformation taking place at the crack tip keeps the stresses finite. An impression of the size of the crack tip plastic zone can be obtained by determining to which distance r_p from the crack tip the elastic stress σ_{yy} , is larger than the yield stress σ_{ys} (Figure. 1.6a), Substituting $\sigma_{yy} = \sigma_{ys}$ into Equation (1.1) for σ_{yy} and taking the plane $\theta = 0$, it follows that:

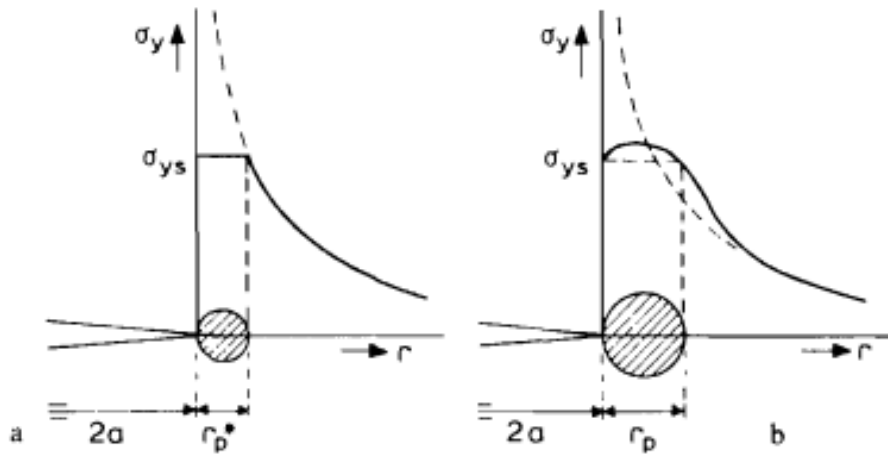


Figure 1.6: Plastic zone at crack tip (a) Assumed stress distribution. (b). Approximate stress distribution

$$\sigma_{yy} = \left(\frac{K_I}{\sqrt{2\pi r_p}} \right) = \sigma_{ys} \quad \text{or} \quad r_p = \frac{K_I^2}{2\pi\sigma_{ys}^2} = \frac{\sigma^2 a}{2\pi\sigma_{ys}^2} \quad (1.3)$$

In reality the plastic zone is somewhat larger (Figure 1.6b). It may suffice here to point out that r_p can be directly expressed as a function of the stress intensity factor and the yield stress. In a foregoing paragraph it was stated that elastic cracks of different sizes but with the same K_I have similar stress fields. The question arises whether this argument still holds if plastic deformation occurs. Cracks loaded to the same K_I have plastic zones of equal size according to Equation (1.3). Outside the plastic zone the stress field will still be the same. If the two cracks have equal plastic zones and the same stresses acting at the boundary of the zone, then the stresses and strains within the plastic zone must be equal. In other words the stress intensity factor is still likely to determine the stress field. It also determines what occurs inside the plastic zone. K is a measure for all stresses and strains. Crack extension will occur when the stresses and strains at the crack tip reach a critical value. This means that fracture must be expected to occur when K_I reaches a critical value K_{Ic} . The critical K_{Ic} may be expected to be a material parameter. One can take a plate with a crack of known size and pull this plate to fracture in a tensile machine. From the fracture load the failure stress σ_c can be calculated. Then it follows that the critical value of the stress intensity factor at the moment of failure is given by:

$$K_{Ic} = \sigma_c \sqrt{\pi a} \quad (1.4)$$

If K_{Ic} is a material parameter the same value should be found by testing another specimen of the same material but with a different size of the crack. Within certain limits this is indeed the case. On the basis of this K_{Ic} value the fracture strength of cracks of any size in the same material can be predicted. It can also be predicted which size of crack can be tolerated in the material if stressed to a given level.

In reality the situation is slightly more complicated. First of all the used expression for the stress intensity factor is valid only for an infinite plate.

$$K_{Ic} = \sigma_c \sqrt{\pi a} f \left(\frac{a}{W} \right) \quad (1.5)$$

where W is the plate width. The function $f(a/W)$ has to be known before K_{Ic} can be determined. Of course, $f(a/W)$ approaches unity for small values of a/W . Secondly, a restriction has to be made as to the transverse strains in the plate. A consistent K_{Ic} value can only be obtained from a test if the displacements in the thickness direction of the plate are sufficiently constrained, i.e. when there is a condition of plane strain. This occurs when the plate has a large enough thickness. If deformations in the thickness direction can take place freely (plane stress situation) the critical stress intensity factor depends upon plate thickness. K_{Ic} is a measure for the crack resistance of a material. Therefore K_{Ic} is called the "plane strain fracture toughness", Materials with low fracture toughness can tolerate only small cracks. The size of crack that can be tolerated in the materials before the strength has decreased to half the original strength can be determined from:

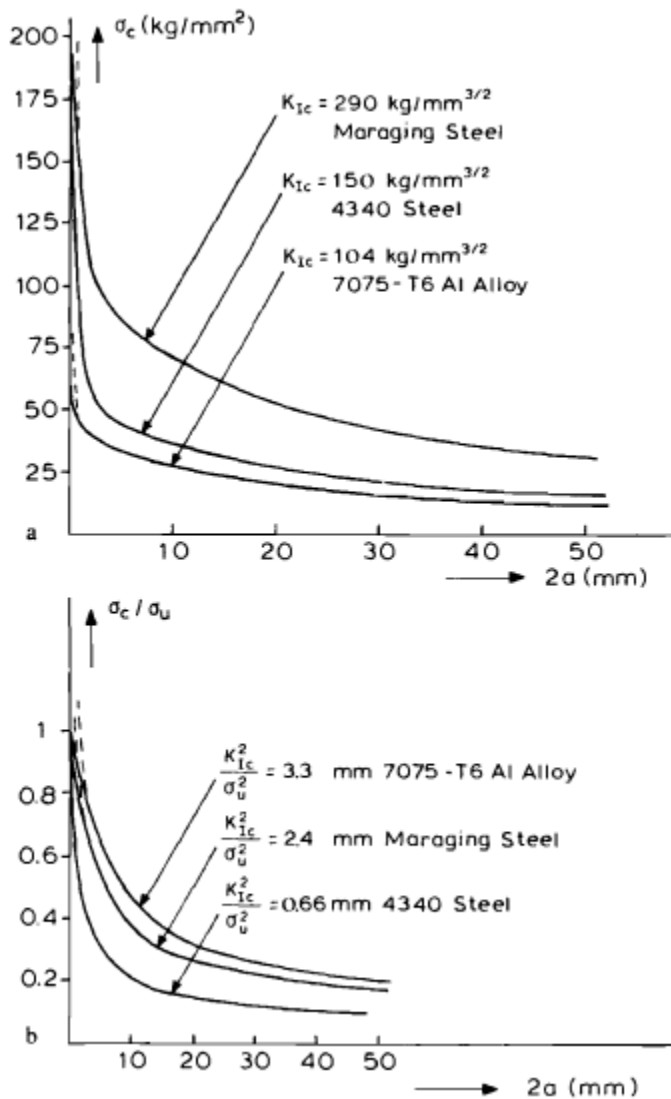


Figure 1.7 Crack toughness of three high strength materials

(a) Residual strength as a function of crack size: (b) Relative residual strength

$$\sigma_c = \frac{K_{IC}}{\sqrt{\pi a}} = \frac{\sigma_u}{2} \text{ or } a = \frac{K_{IC}^2}{\pi \sigma_u^2} \quad (1.6)$$

σ_u is the tensile strength. One finds that a crack of $2a = 1.67\text{mm}$ can be tolerated in the 4340 ($\sigma_u = 1820\text{ MN/m}^2, \sigma_{ys} = 1470\text{ MN/m}^2, K_{IC} = 46\text{ MN/m}^2$) steel, whereas the Maraging 300 ($\sigma_u = 1850\text{ MN/m}^2, \sigma_{ys} = 1730\text{ MN/m}^2, K_{IC} = 90\text{ MN/m}^2$) steel allows a crack of $2a = 6.06\text{ mm}$ and the 7075-T6 aluminium alloy ($\sigma_u = 560\text{ MN/m}^2, \sigma_{ys} = 500\text{ MN/m}^2, K_{IC} = 32\text{ MN/m}^2$) $2a = 8.84\text{ mm}$.

In [Figure 1.7\(a\)](#) the residual strength of the three materials is plotted as a function of crack Length. These curves follow from $\sigma_c = K_{IC}/\sqrt{\pi a}$. The consequence of this formula is that σ_c becomes infinite if a approaches zero. In reality the curve must go to $\sigma_c = \sigma_u$ at $a = 0$. Obviously the material with the highest fracture toughness has the highest residual strength. If the fracture strength is plotted as a fraction of the original (crack free) strength, σ_c/σ_u , the picture is completely different ([Figure 1.7\(b\)](#)). The aluminium alloy tolerates longer cracks than the other materials for a percentage-wise equal loss in strength. This is due to the fact that the aluminium alloy has the highest ratio of toughness to tensile strength (indicated in [Figure 1.7\(b\)](#)).

Supplementary Lectures

Stress Analysis of Crack

1.1 Introduction

For certain cracked configuration subjected to external forces, it is possible to derive closed form expressions for the stress in the body, assuming the isotropic linear elastic material behaviour. If we define a polar coordinate axis with the origin at the crack tip ([Figure 1.1](#)), it can be shown that stress field in any linear elastic cracked body is given by

$$\sigma_{ij} = \left(\frac{k}{\sqrt{r}}\right) f_{ij}(\theta) + \sum_{m=0}^{\infty} A_m r^{\frac{m}{2}} g_{ij}^{(m)}(\theta) \quad (1.1)$$

σ_{ij} = the stress tensor., r and θ defined in the [Figure 1.1](#), k = constant., f_{ij} = dimensionless function of θ in the leading term. For the higher order terms, A_m is the amplitude and $g_{ij}^{(m)}$ is the dimensionless function of θ for the m th term. The higher order terms depend on geometry, but the solution for any given configuration contains the

leading term that is proportional to $1/\sqrt{r}$. As $r \rightarrow 0$, the leading term approaches to infinity. Thus the stress near the crack tip varies with $1/\sqrt{r}$, regard less of the configuration of the cracked body. It can also be shown that the displacement near the crack tip varies with \sqrt{r} . The eqn. 1.1 describes the stress singularities, since stress is asymptotic to $r = 0$ [1].

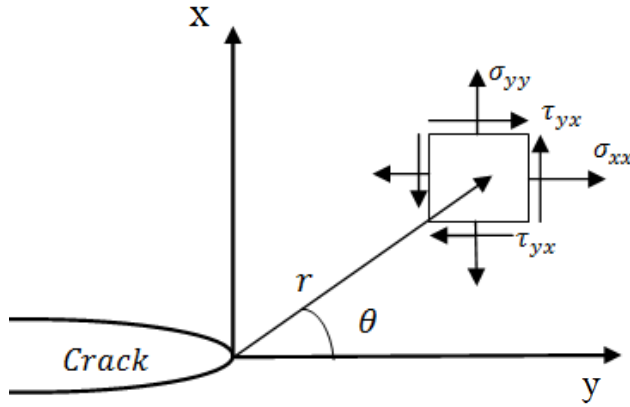


Figure 1. 1:Definition of cordinate axis ahead of crack tip.The z axis is normal to the page.

There are various of techniques for analysing the stress in cracked bodies. The various techniques include the solutions given by Westerguard[2] Irwin[3] and Williams [4], which were among the first ones to publish the solutions. But all the techniques involved ,at last lead to the common solution similar to the general solution given by eqn. 1.1.

1.2 Stress Intensity Factor

Irwin [3] introduced the concept of stress intensity factor. Each mode of loading produces the $1/\sqrt{r}$ singularity at the crack tip, but the proportionality constant k and f_{ij} (eqn. 1.1) depend on the mode. As from the general stress field equation eqn. 1.1, k is replaced by the stress intensity factor K , where $K = k\sqrt{2\pi}$. From the solutions given for the crack tip stresses given by Westergaard [2], or Williams [4]. with $\theta = 0$, we have

$$\left\{ \begin{array}{l} \sigma_{xx} = \frac{K_I}{\sqrt{2\pi r}} \cos\left(\frac{\theta}{2}\right) \left[1 - \sin\left(\frac{\theta}{2}\right) \cos\left(\frac{3\theta}{2}\right) \right] \\ \sigma_{yy} = \frac{K_I}{\sqrt{2\pi r}} \cos\left(\frac{\theta}{2}\right) \left[1 + \sin\left(\frac{\theta}{2}\right) \cos\left(\frac{3\theta}{2}\right) \right] \\ \tau_{xy} = \frac{K_I}{\sqrt{2\pi r}} \cos\left(\frac{\theta}{2}\right) \sin\left(\frac{\theta}{2}\right) \cos\left(\frac{3\theta}{2}\right) \\ \sigma_{zz} = 0 \quad (PSS) \\ \sigma_{zz} = \nu(\sigma_{xx} - \sigma_{yy}) \quad (PSN) \end{array} \right. \quad (1.2)$$

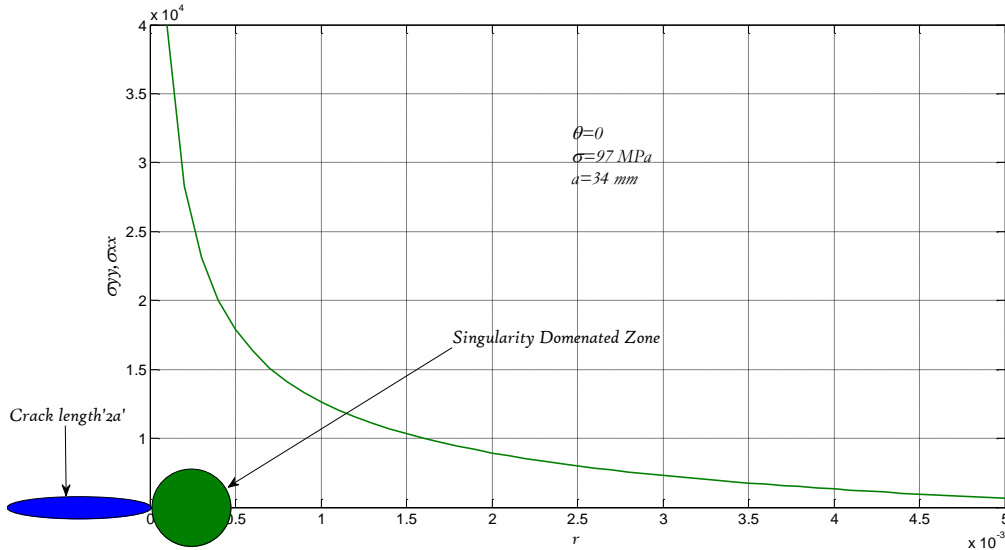


Figure 1.2: Stress normal to the Crack Plane in Mode I

When $\theta = 0$, the shear stress is zero, which means that the crack plane is a principal plane for pure *Mode I* loading. *Figure 1.2* is a plot of σ_{yy} , σ_{xx} , the stress normal to the crack plane vs distance from the crack tip. The $\sigma_{xx} = \sigma_{yy} = K_I / \sqrt{2\pi r}$ is valid only near the crack tip, where the $1/\sqrt{r}$ singularity dominates the stress field. The stress intensity factor defines the amplitude of the crack tip singularity. That is the stress near the crack tip increase in proportion to K, the stress intensity factor which completely defines the crack tip conditions, if K is known, it is possible to solve for all components of stress, strain and displacement as a function of r and θ .

Principal stresses

The in-plane principal stresses σ_1 and σ_2 obtained from in eqn. 1.2 for *Mode I* loading are

$$\left\{ \begin{array}{l} \sigma_1 = \frac{K_I}{\sqrt{2\pi r}} \cos \frac{\theta}{2} \left(1 + \sin \frac{\theta}{2} \right) \\ \sigma_2 = \frac{K_I}{\sqrt{2\pi r}} \cos \frac{\theta}{2} \left(1 - \sin \frac{\theta}{2} \right) \\ \sigma_3 = 0 \quad (PSS) \\ \sigma_3 = \nu(\sigma_1 + \sigma_2) \quad (PSN) \end{array} \right. \quad (1.3)$$

The equation for stress field ahead of crack obtained from the Williams and Westergaard solution converges to common solutions. These equations include the stress intensity factor which will help defining the amplitude of the crack tip singularity and the crack tip conditions around the crack at different angles θ . The stress intensity factor discussed above is strictly valid for an infinite plate.

The geometry of finite size specimens has an effect on the crack tip stress field, and so expressions for stress intensity factors have to be modified by the addition of correction factors to enable their use in practical problems [5]. As a crack size increases, the outer boundaries began to exert an influence on the crack tip. In such

a case closed form stress intensity factor solution is not possible. Consider a cracked plate subjected to a remote tensile stress. The effect of finite width on a crack tip stress distribution, which is represented by the lines of forces, the local stress is proportional to the spacing between lines of forces. Since the tensile stress cannot be transmitted through a crack, the lines of forces are diverted around the crack, resulting in the local stress concentration. In the infinite plate, the lines of forces at a distance W from the crack centerline has a force component in x and y direction. In finite width boundary condition is to assume a periodic array of collinear cracks in an infinite plate of crack length $2a$ and the remote stress applied is σ The Mode I stress intensity factor for this situation is given by [1],

$$K_I = \sigma\sqrt{\pi a} \left[\frac{2W}{\pi a} \tan\left(\frac{\pi a}{2W}\right) \right]^{1/2} \quad (1.4)$$

The stress intensity approaches the infinite plate value as a/W approaches zero K_I is asymptotic to $a/W = 1$. More accurate solutions for a through crack in a finite plate have been obtained from finite-element analysis, solutions of this type are usually fit to a polynomial expression. One such solution [6] is given by

$$K_I = \sigma\sqrt{\pi a} \left[\sec\left(\frac{\pi a}{2W}\right)^{1/2} \right] \left[1 - 0.025\left(\frac{a}{W}\right)^2 + 0.06\left(\frac{a}{W}\right)^4 \right] \quad (1.5)$$

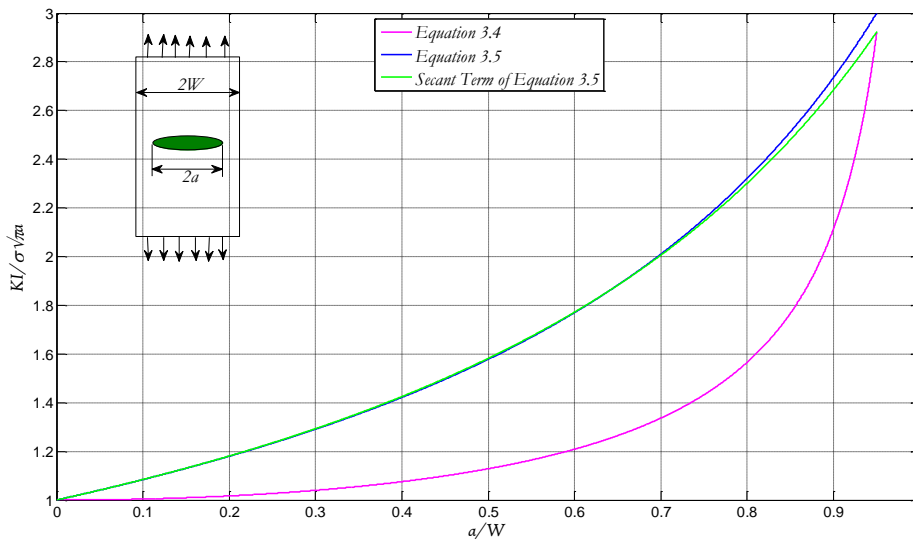


Figure 1.4: Comparison of finite width correction for centre cracked plate in tension

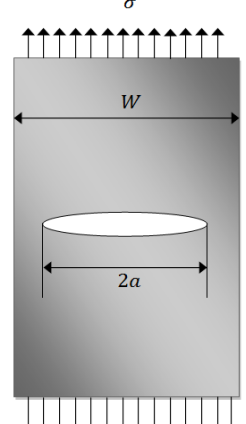
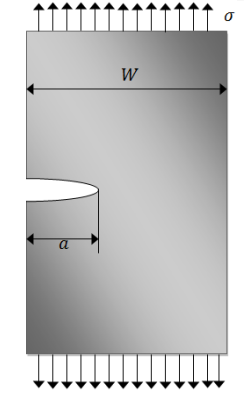
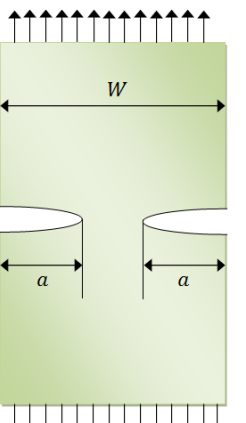
Figure 1.4 compares the finite width corrections in eqn. 1.4 and eqn. 1.5. The secant term (without the polynomial term) in eqn. 1.5 is also plotted. Eqn. 1.5 agrees with the finite-element solution to within 7% for $a/W < 0.6$. The secant correction is much closer to the finite element solution, the error is less than 2% for $a/W < 0.9$. A general form of a modified expression is $K_I = \sigma\sqrt{\pi a} Y$, where Y is the geometry factor and is a function of a/W , i.e., $f(a/W)$

1.3 Stress Intensity Factor for some common Geometries

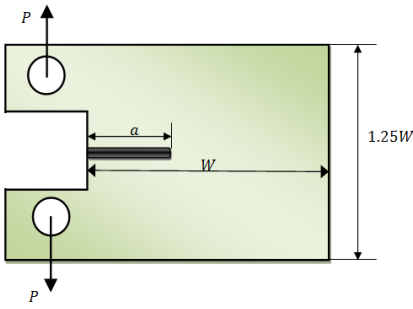
The stress intensity factors for some commonly used fatigue testing specimen and crack configuration are shown here. These results are from hand books of Tada, Paris and Irwin [8], where further details and derivations can be found. The specimen geometry for centre crack is shown in the *Table 1.1* For this specimen there are various expressions for stress intensity factor e.g. as shown by Irwin for one of the collinear cracks with interspacing W in an infinite plate. A numerical solution was obtained by Isida [cited in 5]. The geometric correction factor $f(a/W)$ was derived as a 36 term power series. However Brown [cited in 5] found a 4 term approximation to this power series with 0.5% accuracy for $a/W \leq 0.35$. this approximation. The compressive stresses acting along the crack flanks in a uniaxially loaded plates ($\sigma_{xx} = -\sigma$) and have a closing effect on the crack in a centre cracked specimen. This closing effect is absent in the case of edge cracks, since σ_{xx} at the free edge must be zero. Therefore, for equal crack length a and stress σ , the edge crack shows a larger crack opening at the edge than a centre crack does in the middle. Thus there is a stress raising effect of the free edge. This effect has been estimated to be about 12%, i.e. an increase of σ by 12% would be needed to obtain the same crack opening for centre crack. Thus for an edge crack [5], $K_I = 1.12\sigma\sqrt{\pi a}$.

This closing effect is absent in the case of edge cracks, since σ_{xx} at the free edge must be zero. Therefore, for equal crack length a and stress σ , the edge crack shows a larger crack opening at the edge than a centre crack does in the middle. Thus there is a stress raising effect of the free edge. This effect has been estimated to be about 12%, i.e. an increase of σ by 12% would be needed to obtain the same crack opening for centre crack. Thus for an edge crack [5], $K_I = 1.12\sigma\sqrt{\pi a}$. For longer cracks the finite geometry results in stress enhancement. Correction factors have to take both the free edge effect and finite geometry effect into account. This is reflected in the following very accurate expression. *Table 1.1* lists stress intensity solutions for several different configuration. The stress intensity factor for several common configurations are plotted in *Figure 1.5*

Table 1. 1: Solutions for test specimens

<p>Centre Cracked Specimen</p> 	$Y = 1 + 0.256 \left(\frac{a}{W}\right) - 1.152 \left(\frac{a}{W}\right)^2 + 12.2 \left(\frac{a}{W}\right)^3$
<p>Single Edge Cracked Specimen</p> 	$K_I = 1.12\sigma\sqrt{\pi a}$ $Y = 1.122 - 0.231 \left(\frac{a}{W}\right) + 10.550 \left(\frac{a}{W}\right)^2 - 21.710 \left(\frac{a}{W}\right)^3 + 30.382 \left(\frac{a}{W}\right)^4$
<p>Double Edge Cracked Specimen(DECS)</p> 	$Y = \frac{1.122 - 1.122 \left(\frac{a}{W}\right) - 0.820 \left(\frac{a}{W}\right)^2 + 3.768 \left(\frac{a}{W}\right)^3 - 3.040 \left(\frac{a}{W}\right)^4}{\sqrt{1 - \frac{2a}{W}}}$

Compact Tension Specimen.(CTS)



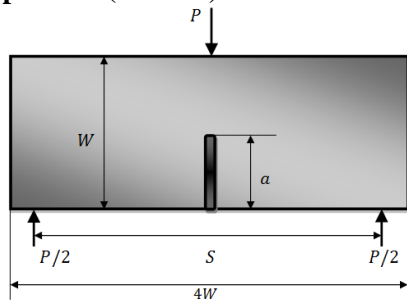
$$K_I = \frac{P}{BW^{\frac{1}{2}}} Y$$

B is the thickness of specimen.

Y

$$Y = \frac{\left(2 + \frac{a}{W}\right) \left\{0.886 + 4.64 \left(\frac{a}{W}\right) - 13.32 \left(\frac{a}{W}\right)^2 + 14.72 \left(\frac{a}{W}\right)^3 - 5.6 \left(\frac{a}{W}\right)^4\right\}}{\left(1 - \frac{a}{W}\right)^{\frac{3}{2}}}$$

Single Edge Cracked Bend Specimen(SECBS)



$$K_I = \frac{PS}{BW^{\frac{3}{2}}}$$

B is the specimen thickness.

$$Y = \frac{3 \left(\frac{a}{W}\right)^{\frac{1}{2}} \left[1.99 - \frac{a}{W} \left(1 - \frac{a}{W}\right) \left\{2.15 - 3.93 \left(\frac{a}{W}\right) + 2.7 \left(\frac{a}{W}\right)^2\right\}\right]}{2 \left(1 + 2 \frac{a}{W}\right) \left(1 - \frac{a}{W}\right)^{\frac{3}{2}}}$$

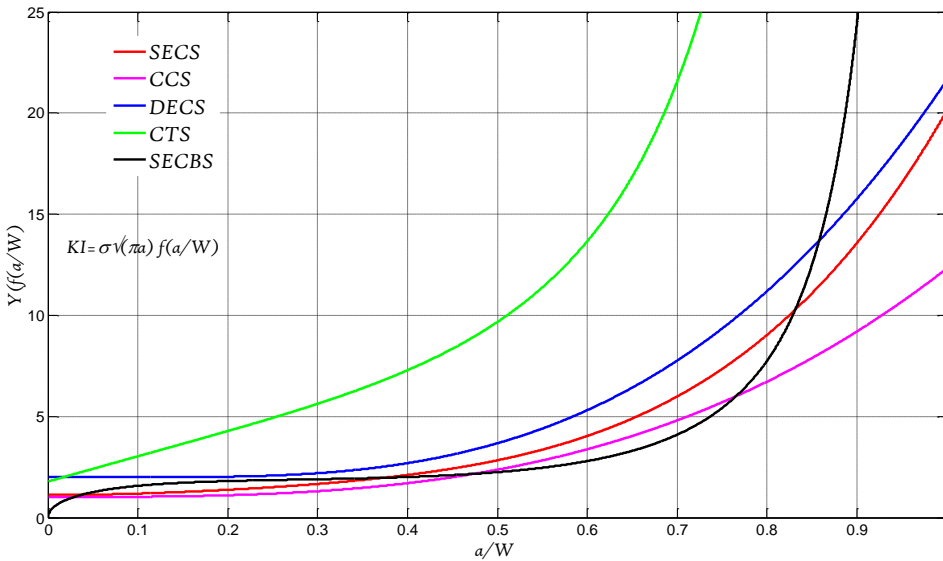


Figure 1.5: Stress intensity solution for several common geometries.